JSEE Vol. 23, No. 2, 2021 DOI: 10.48303/jsee.2023.555428.1018

Research Paper

Assessment of a 475-Year Scenario Earthquake Loss for Residential Buildings in District 2 of Tehran Municipality, Iran

Niloofar Kazemi Asl [1], Hooman Motamed[2*], Mohsen Fazlavi[3] and Mahdi Mahdikhani[4]

1. M.Sc. Student, Faculty of Technical and Engineering, Imam Khomeini International University, Qazvin, Iran
2. Assistant Professor, Risk Management Research Center, International Institute of Earthquake Engineering and Seismology (IIEES), Tehran, Iran,
*Corresponding Author; email: h.motamed@iiees.ac.ir,
3. Assistant Professor, Technical and Vocational University (TVU), Tehran, Iran
4. Assistant Professor, Civil Engineering, Faculty of Technical and Engineering, Imam Khomeini International University, Qazvin, Iran

Received: 08/06/2022
Revised: 08/12/2022
Accepted: 10/01/2023

ABSTRACT

Tehran, the capital city of Iran, is a dense city with more than 12 million dynamic population. The city is located next to the seismically active zone of the Alborz Mountains, with many active faults surrounding it. Because of Tehran's significant economic and political position at the national level, earthquakes in this city or its vicinity could eventually affect the entire country. This can explain how important the identification and assessment of seismic risk in this city can be. In this study, an OpenQuake-engine has been employed to quantify the earthquake risk of one of the districts of Tehran. Initially, a probabilistic hazard assessment was carried out for Tehran; then, after disaggregating the result of a 475-year PSHA, the main contributing earthquake scenario was selected as the hazard input. In addition, an exposure model was developed for the residential buildings of the study area, indicating building typology and locations. Further, a set of fragility and vulnerability functions that are consistent with the exposure model was selected from past studies. Finally, the seismic loss for residential buildings in District 2 of Tehran municipality was assessed in the event of the 475-year hazard scenario. The results show the complicated intensity and spatial distribution of damages and losses in various subdivisions of the study area. Such analysis can provide essential information for disaster management decision-makers to become prepared for possible future events.

Keywords:
Earthquake losses; Seismic hazard assessment; Exposure; Vulnerability; Seismic risk; Tehran

1. Introduction

In recent decades, population growth and migration from rural areas to large cities have caused rapid and uncontrolled expansion of urban areas. This population growth has led to the rise of the vulnerability of cities to natural hazards in terms of increased risk. The widening gap between engineering knowledge and construction practice, as well as the focus of disaster management systems on mere emergency response, have intensified the situation ([1-2]).

Earthquakes are among the most devastating natural hazards that can give rise to considerable human and economic losses. Since 1980, earthquakes have accounted for 12.2% of all catastrophic natural perils worldwide, contributing to 56.2% of all casualties and 25.2% of economic losses in

total [3]. They have resulted in more than 800,000 fatalities, 1.4 million injuries, and 30 million people being made homeless. Additionally, around USD 950 billion in financial losses have been inflicted by damaging earthquakes during the same period [4].

Tehran, the capital of Iran, is a highly dense and populated city with a more than 12 million dynamic population [5]. Tehran is Iran's political and economic capital, and its destruction could disrupt the supply-demand chain across the country. Many destructive earthquakes occurred in Tehran over the past centuries. Historical sources indicate the destruction of Tehran due to six catastrophic earthquakes, the earliest of which occurred in the 4th century BC ([6-7]) and the most recent in 1830. The city is located in the vicinity of the seismic zone of the Alborz Mountains, and many active faults surround it [8]. Tehran is enclosed by the main active faults of the North Tehran Fault and Mosha in the north, and Kahrizak, North Rey, South Rey, Eyvanaki, Garmsar and Pishva faults in the south.

Previously, many researchers have investigated various elements of seismic risk in Tehran. As one of the earliest studies, Ghafory-Ashtiany and Tavakoli estimated the PGA of 75- and 475-year return period earthquakes, employing probabilistic hazard assessment [9]. In another research, Ghodrati-Amiri et al. [7] carried out a probabilistic seismic hazard assessment of Tehran, which estimated the Peak Ground Acceleration (PGA) on the bedrock for 475 and 950-year return periods. They used a logic tree method to weigh three attenuation relationships in their study. In 2005, Zare [10] estimated the Pick Ground Acceleration for the return period of 75, 475, and 2475 years; similarly, in 2006, Mirazaei [11] performed a probabilistic hazard assessment for capital for 50 and 475 years return period.

In 2009, further investigation was made by Zafarani et al. [12], where they suggested a stochastic physical model and applied it to Tehran city. In that study, the PGA in some earthquake scenarios exceeded 0.7g. In 2010, Nowroozi et al. [8] examined the potential seismicity of major faults around Tehran and calculated the intensity measures in a grid of points. Four years later, Wang and Taheri [13] carried out another study regarding seismic risk assessment in Tehran. This study presented a new hazard map for Tehran by employing deterministic seismic hazard analysis.

Similarly, Bastami and Kosari [14] investigated the region's seismic hazard using the Gumbel distribution method and estimated the distribution of bedrock PGA. In 2015, Boostan et al. [15] presented a new probabilistic seismic hazard assessment model based on fuzzy sets theory and applied it to Tehran. More recently, Firuzi et al. [16] conducted a stochastic hazard analysis for Tehran using a Monte Carlo simulation methodology. The assessment included the development of a robust approach to quantify the seismic hazard by considering the dynamic soil response to calculate PGA for the return periods of 475 and 2475 years. In 2021, Kowsari and Ghasemi [17] studied the probabilistic seismic hazard analysis for the North Tehran Fault scenario using time-independent and time-dependent approaches. The results showed that the ground motion values increased by 20-40% and 10-20% for the 1-in-475 and 1-in-2475-year events, respectively, particularly in the near-fault range.

In studies concerning the development of exposure models and building typology, Mansouri et al. [18] presented a classification for the common Iranian buildings using the European Macro-seismic Scale (EMS 98). In a similar study in 2015, Sadeghi et al. [19] presented another classification for Iranian residential buildings by investigating the prevalent residential buildings in urban and rural areas in Iran. Again in 2019, Motamed et al. [20] proposed 23 classes for Iranian buildings by examining the available census data based on information on construction materials, structure height, lateral load resisting systems, and construction year. More recently, Fallah-Tafti et al. [21] divided all Iranian buildings into 19 general categories in terms of structural type, structure quality, and building height.

In terms of the seismic vulnerability of buildings, a pioneer study carried out by Tavakoli and Tavakoli [22] suggested an empirical vulnerability function for 'semi-engineered' buildings based on the loss data collected after the Manjil-Rudbar earthquake of 1990. Ten years later, JICA developed vulnerability curves for nine types

of common buildings in Tehran using the proposed curve by Tavakoli and Tavakoli [22], guidelines of ATC-13, and expert opinion [23]. In another study in 2014, Mansouri et al. [18] proposed a set of fragility curves for nine types of Iranian buildings in Iran under the EMME (EMME: Earthquake Model of the Middle East) project utilizing a parametric method developed by EMS-98. There are other sets of fragility/vulnerability curves suggested for Iranian buildings by other researchers. For instance, Ranjbaran and Hosseini [24] and Kazemi et al. [25] proposed relations between the different classes of buildings' damage and ground motion parameters. Most of these studies are considered by Sadeghi et al. [19] and Pakdel-Lahiji et al. [26] in developing seismic vulnerability curves for typical Iranian buildings. In the latest research published by Fallah-Tafti et al., a set of fragility curves were developed by allocating weights to then available fragility functions that could represent Iranian building typology [21].

As said, past studies show that most of the country faces a high level of seismicity. This degree of seismic hazard, when combined with dense vulnerable urban areas, this degree of seismic hazard will result in worrying the size of earthquake risks, particularly in large and medium-sized cities. To manage the risk, the disaster risk management organizations such as the National Disaster Management Organization (NDMO), Planning and Budget Organization (PBO), the Housing Foundation, the Red Crescent, and local municipalities will require insight into the extent and size of the impact to inform their decisions and investments. Despite the significance of the matter, few studies were conducted on the assessment and quantification of earthquake risk in Iran. The present study aims to perform a scenario risk assessment in District 2 of Iran's capital city, Tehran, and examines the physical and financial impact of a major seismic event in this district. Because the size and population of the study area are comparable to other large-size cities in the country, the results could be used by other local governments in forming an understanding of how other similar-size urban areas could be affected by large-scale seismic events in the future.

This paper aims to assess seismic hazard and risk (loss) in District 2 of Tehran as a prerequisite analysis for disaster risk management planning in urban areas of similar size and seismicity level. In this study, several components of an earthquake risk model, namely hazard, vulnerability and exposure, have been either selected from credible studies or developed specifically for the geography under assessment. Finally, risk components were combined to generate a spatial distribution of losses for a 475-year scenario in the pilot area.

2. Development of Seismic Hazard and Risk Model

For assessing risk, three main components should be prepared: a seismic hazard analysis to evaluate ground shaking intensity across the study area, an exposure model which shows the spatial distribution of the value at risk, and vulnerability functions to relate the hazard intensity to the probability of loss exceedance for each type of assets. This section describes the procedure for developing the required risk components and then shows how these modules are combined to quantify seismic risk in District 2 of Tehran.

2.1. Seismic Hazard

In finding the appropriate earthquake scenario for a 475-year period, as one of the risk assessment inputs, it is necessary first to conduct a probabilistic seismic hazard analysis (PSHA) for the region and then select the event with the most contribution to a 1-in-475-year hazard using the disaggregation process. To this end, as the first step, historical and instrumental seismic events were collected within the 200 kilometers distance from the centroid of Tehran city. Then, the active faults were identified in the selected region, and the seismic sources model was developed by delineating the region using seismotectonic maps, seismicity, and engineering judgments. The resulted seismic source model includes 13 area zones containing active faults ($L1$ - $L13$) and 9 area zones containing background seismicity ($Z1$ - $Z9$). Two main methods, namely Gardner and Knopoff [27], and Uhrhammer [28] were employed to eliminate foreshocks and aftershocks from the earthquake catalog in the study region. The declustering methods reduced the original number of events

from 447 to 263 and 330 events for Gardner-Knopoff and Uhrhammer, respectively (see Figure 1).

The completeness magnitude (mc) is the minimum earthquake magnitude above which seismograph stations have completely detected the earthquake events. This parameter should be available before determining the seismicity parameters of each seismic zone. The methodology suggested by Wiemer and Wyss [29] was used to calculate Mc. Results show that Mc is equal to 4.7, 4.5 and 4 for the 1900-1963, 1963-2000, and 2000-2022 periods, respectively. After completing the event catalog, the seismicity parameters were determined utilizing methodologies proposed by Gutenberg-Richter [30] and Kijko [31] for all seismic zones (see Table 1) [27-28].

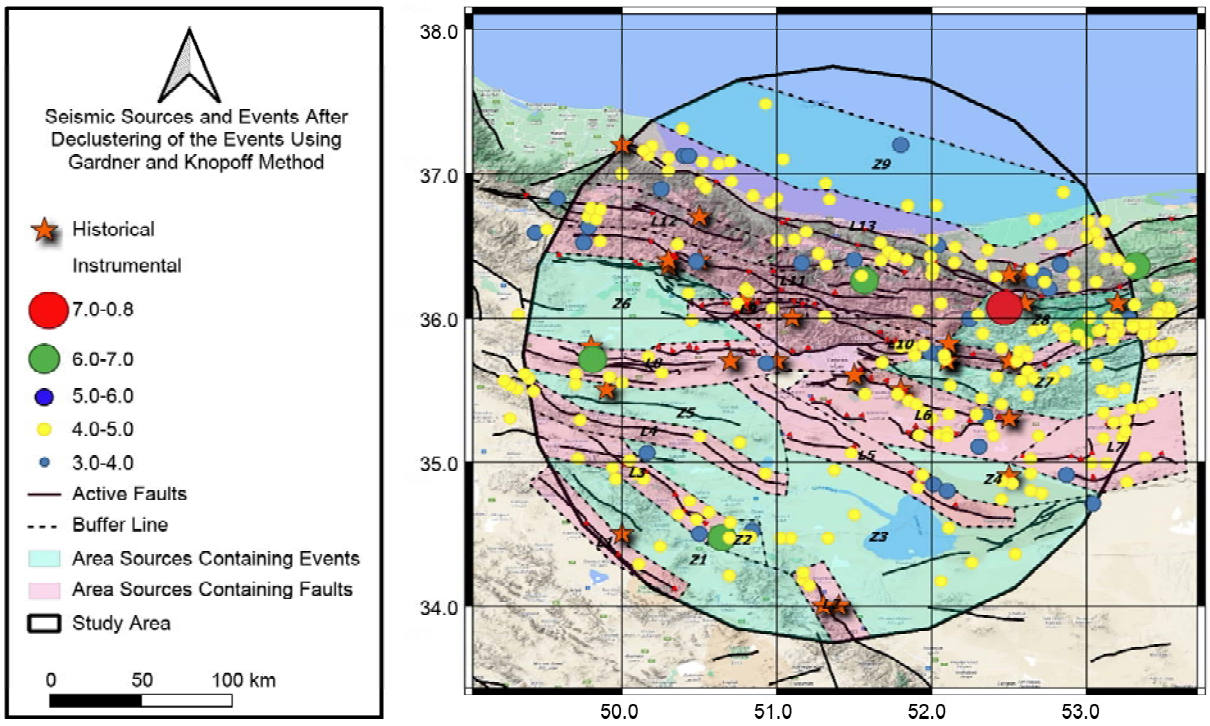

Figure 1. Declustering seismic events using the windowing algorithm proposed by Gardner and Knopoff [27].

Table 1. Seismic parameters calculated for seismic sources based on the catalog declustered using Gardner and Knopoff [27].

Catalog	Seismic Sources	Seismic Parameters Calculated Based on the Kijko Method			Seismic Parameters Calculated Based on the Gutenberg-Richter Method		
		λ_i	b	a_i	λ_i	b	a_i
Gardner and Knopoff [27]	Z1	0.18775	1.18	3.99	0.27133	0.909	3.07
	Z2	0.34135	1.18	4.25	0.47097	0.909	3.31
	Z3	0.75133	1.18	4.60	1.00649	0.909	3.64
	Z4	0.45427	1.18	4.38	0.57071	0.909	3.39
	Z5	0.15361	1.18	3.91	0.19964	0.909	2.94
	Z6	0.18775	1.18	3.99	0.27133	0.909	3.07
	Z7	1.05233	1.18	4.74	1.29874	0.909	3.75
	Z8	1.06287	1.18	4.75	1.43178	0.909	3.79
	Z9	0.63875	1.18	4.53	0.82793	0.909	3.55
	L1	0.03268	1.18	3.23	0.04033	0.909	2.24
	L2	0.11142	1.18	3.77	0.15450	0.909	2.82
	L3	0.30610	1.18	4.21	0.39046	0.909	3.23
	L4	0.16341	1.18	3.93	0.20167	0.909	2.94
	L5	0.12199	1.18	3.81	0.17591	0.909	2.88
	L6	0.51732	1.18	4.43	0.67597	0.909	3.47
	L7	0.46951	1.18	4.39	0.59212	0.909	3.41
	L8	0.19016	1.18	4.00	0.26867	0.909	3.07
	L9	0.06712	1.18	3.55	0.09068	0.909	2.59
	L10	0.74714	1.18	4.59	0.96038	0.909	3.62
	L11	0.27982	1.18	4.17	0.40821	0.909	3.25
	L12	0.13213	1.18	3.84	0.16738	0.909	2.86
	L13	1.69122	1.18	4.95	2.22264	0.909	3.98

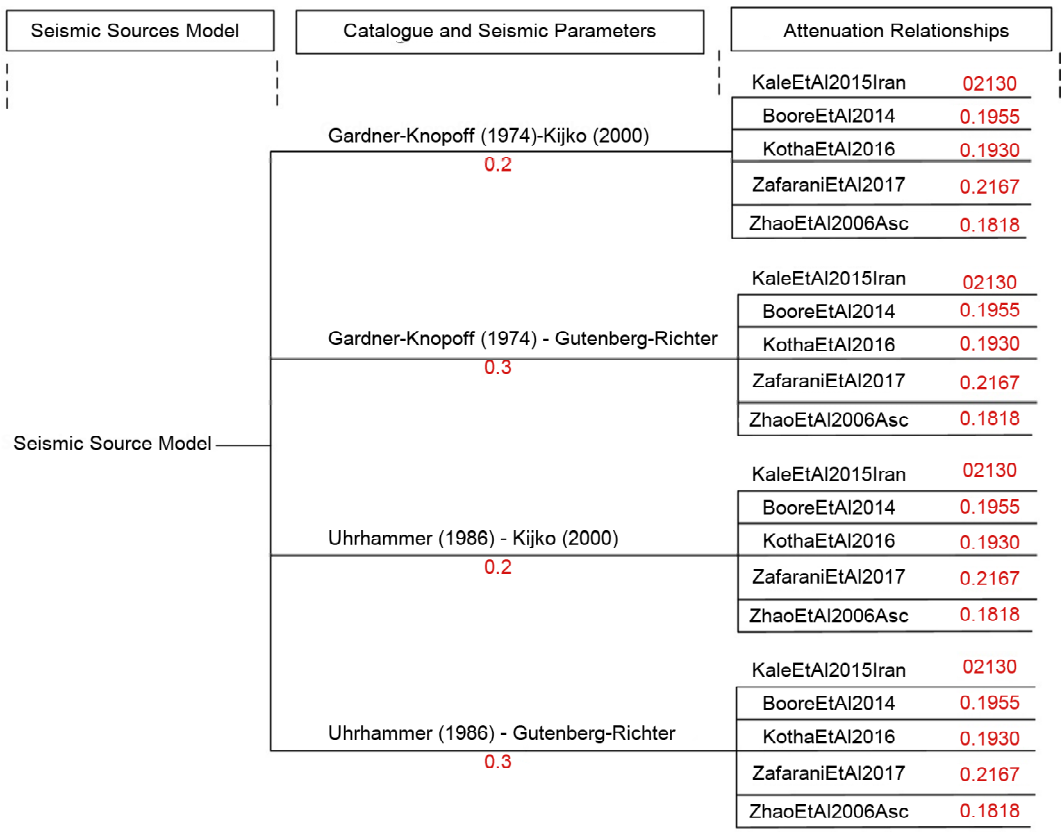

Figure 2. The logic tree of the seismicity model and corresponding weights of the branches.

In the next step, based on the nature of the seismotectonic in the study area, appropriate ground motion prediction equations (GMPEs) are selected. To consider the uncertainty of GMPEs, a combination of local, regional, and global equations was selected. In addition, a logic tree structure, along with weights for each GMPE, was included in the PSHA calculation process. These weights were adopted from a recent study conducted by Firuzi et al. [32].

Figure (2) shows the branching of the logic tree and the weights used. It should be noted that weights for methods used for declustering catalogs and calculating recurrence parameters were determined by engineering judgment.

Since soil layers above the engineering bedrock can amplify the ground motion parameters, the impact of the soil deposits should be incorporated in the calculation of intensity measures [33]. In this regard, the results of a study by the Japan International Cooperation Agency (JICA) on the amplification effect of soil in the city of Tehran were used [34]. In JICA's study, the soil model consists of amplification factors for a grid of 0.0055×0.0055 degrees in Tehran. Finally, a PSHA was carried out using GEM's OpenQuake platform. The results suggest that the expected PGA for the return periods of 475 and 2475 years range from 0.25g to 0.5g for a probability of 1-in-475 and from 0.45g to 0.95g for a probability of 1-in-2475. The distribution of PGA on the soil surface for both exceedance probabilities is shown in Figure (3). As seen, the effect of soil amplification is observed in northern and central Tehran for both results.

The main purpose of this paper is to inform the decisions of disaster management organizations in understanding the nature of the losses and then managing seismic risk in the study area. Therefore, the hazard input of risk analysis should be a single earthquake scenario rather than a combination of many scenarios convoluted by a probabilistic process. In so doing, the results of the PSHA need to be disaggregated to find a single event with the maximum contribution to the chosen probability of exceedance (475-year). The reason for choosing the 475-year return period is its usage in the code 2800 which is used for designing buildings in Iran. The hazard disaggregation process was done using the OpenQuake platform. The disaggregation results indicate that a magnitude 6.1 earthquake

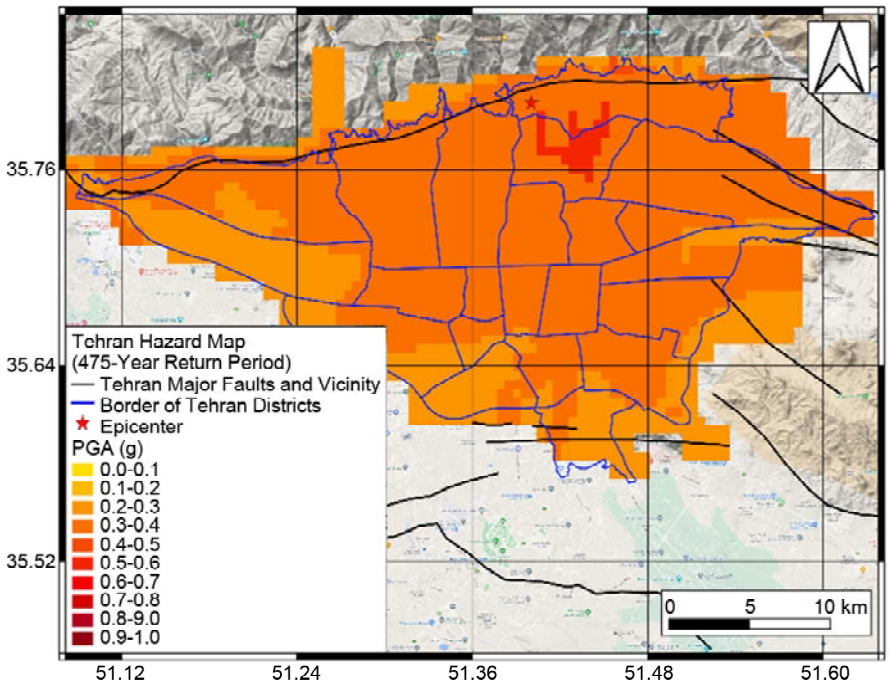

(a) 475 - Years Return Period

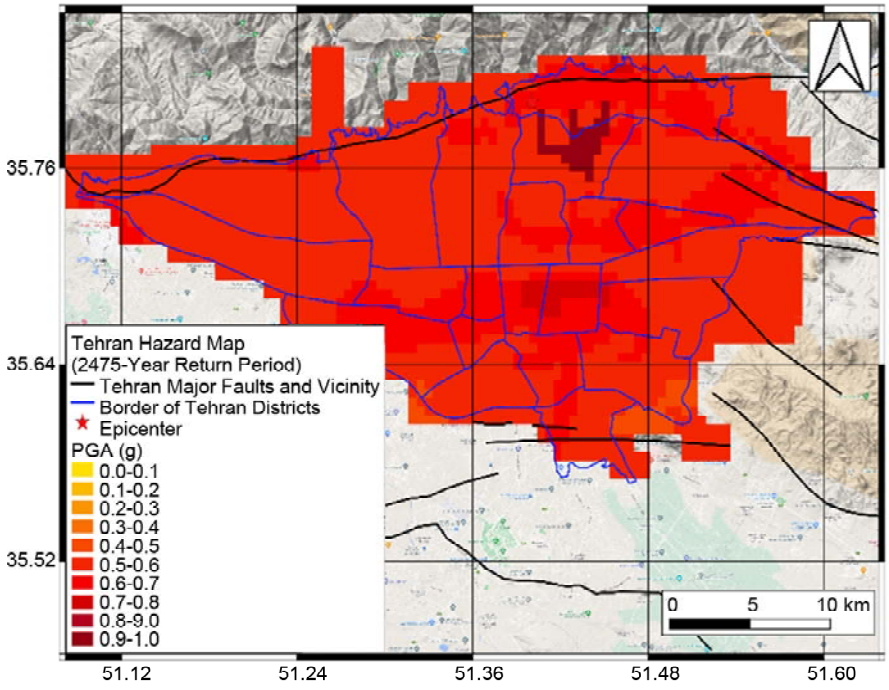

(b) 2475 - Years Return Period

Figure 3. Tehran hazard map.

generated by North Tehran Fault (NTF) is the scenario having the highest contribution to the 1-in-475 hazard to the centroid of District 2 of Tehran. Figure (4) depicts the disaggregation results in terms of epicenter coordinates and the magnitude of possible scenarios.

As shown in Figure (5), the identified scenario was used to estimate the PGA distribution in bedrock and on the soil surface across the city of Tehran. Again, the soil amplification effect is apparent in the northern parts of Tehran (due to its proximity to the epicenter).

The results indicate that the expected PGA for the return periods of 475 and 2475 years are 0.25 g-0.5 g and 0.45 g-0.95 g, respectively. Since the average PGA estimated for Tehran city in other studies is in the range of 0.33 g-0.42 g and 0.47 g-0.9 g for 475 and 2475-year return periods,

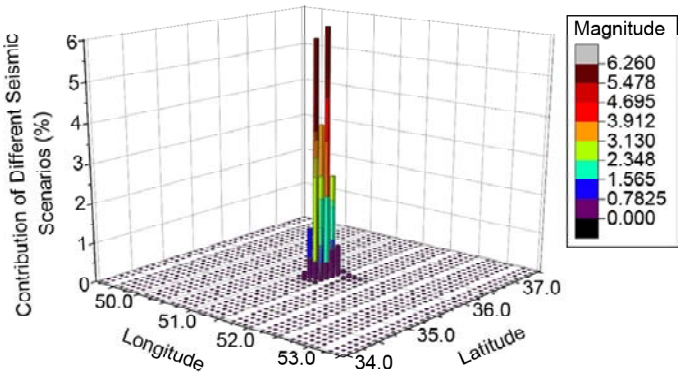

Figure 4. Hazard disaggregation result: probability of exceedance of events due to magnitude and coordination.

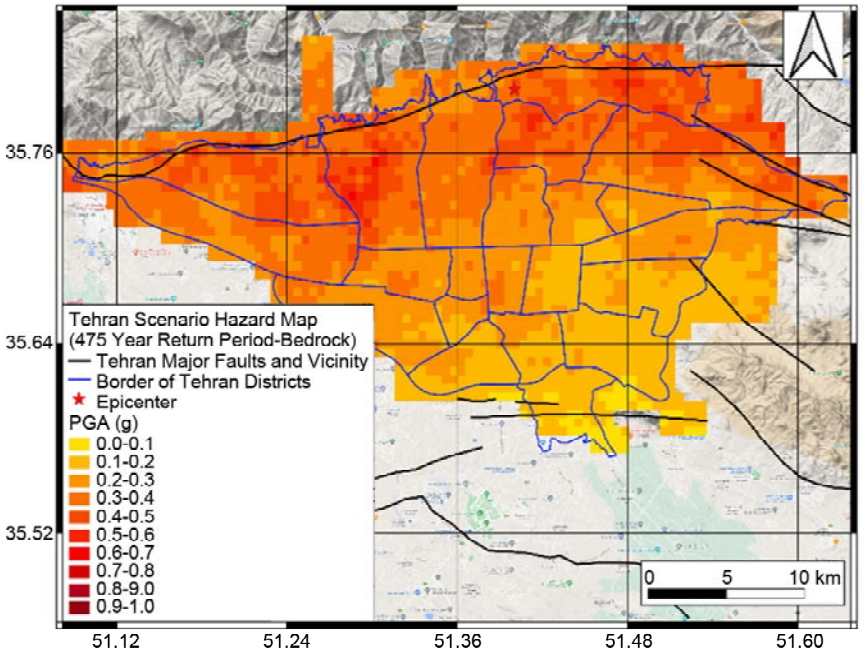

(a) Bedrock

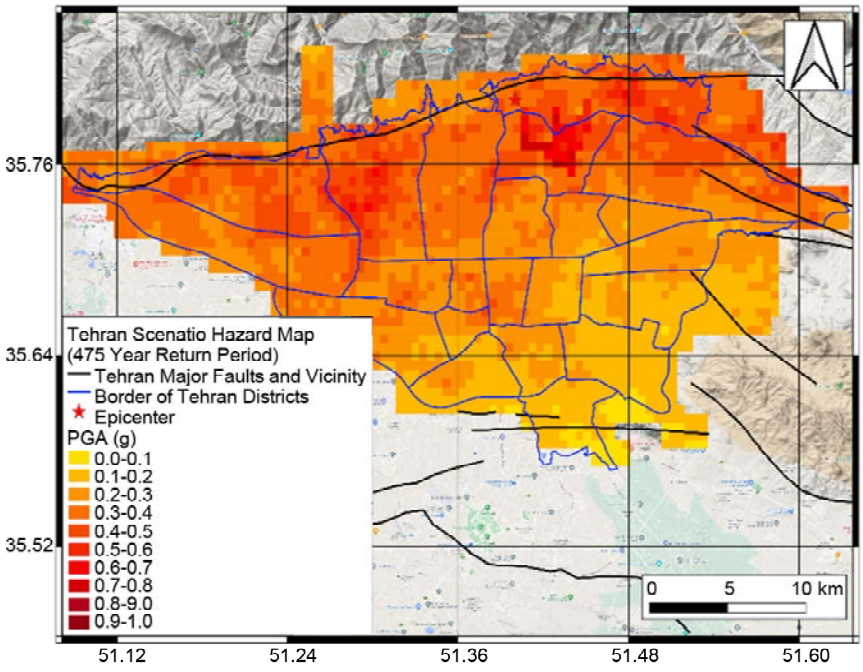

(b) Considering Soil Amplification Factor

Figure 5. Tehran scenario hazard map for 475-year return period.

respectively, the results of the current study have relatively good accuracy in comparison to the other studies [7-17]. However, some discrepancies are mostly different in applied methods, selection of soil model, development of seismic sources model using geological/ tectonic structure, seismicity, and engineering judgments.

2.2. Exposure Model

A building exposure model is a dataset that comprises building typology, the spatial distribution of buildings, the replacement cost, and other supplementary information. The building exposure model used in this risk assessment study was developed in two stages. First, the 2016 housing census (the most recent Census) data containing several fields on the construction material, number of stories, construction year, and their location at the parcel resolution was acquired from the Tehran Disaster Management and Mitigation Organization (TDMMO). To enhance the completeness, accuracy, and consistency of the acquired data, field missions were organized to collect the exact data for random buildings in District 2 of Tehran. The collected data was later used to make informed assumptions for enhancing the quality of the primary exposure model. The residential building data were then classified into different vulnerability classes according to the construction materials, year built, and the number of stories. According to the analysis, the total number of residential buildings in District 2 of Tehran was about 49,980 in 2016. Based on their construction material, the lateral load-resisting system was classified into four classes steel, reinforced concrete, masonry, steel or concrete, and adobe buildings. The masonry class contained further sub-classes: brick and steel, brick and wood, brick and stone, concrete blocks, stone blocks, and wood. In general, adobe buildings are comprised of materials such as adobe and mud, adobe and wood, and others. Table (2) describes how the total number of the district buildings is split into various construction classes. Figure (6) illustrates examples of different

Figure 6. Examples of different construction classes in District 2 of Tehran.

Table 2. General distribution of residential buildings in district 2 of Tehran.

Type of Construction	No. of Dwellings	Percentage
Steel Structures	16931	36.08
Reinforced Concrete Structures	9770	20.82
Masonry	19966	42.55
Steel or Concrete Structures	225	0.48
Adobe	32	0.07

construction classes in the study area.

In the process of exposure model development, recent housing census information was used to define a set of building classifications. Within the residential building stock, masonry buildings (42%) were the predominant type of construction, followed by steel structures (36%), reinforced concrete structures (20%), and other types (less than 2%). The dataset on the building exposure of the study area was not fully complete and lacked construction years. Therefore, we conducted a field survey to obtain and complete the exposure data. For this purpose, 100 buildings were selected randomly sampled across the District 2 of Tehran city and their construction year data were collected by interviewing the owners. The results were used to establish the age distribution of each construction type (masonry, steel, and concrete). Then this distribution was utilized to build three vulnerability curves for buildings without age attributes of the mentioned constructions.

The building can also be classified according to its construction year, which is a proxy parameter for the quality of construction. This classification is made based on dates when different versions of the Iranian code of practice for the seismic-resistant design of buildings called Standard No. 2800 were enforced for implementation by the law and housing census data collection periods. As a result, buildings were divided into three quality levels based on the periods in which they were constructed: low-quality (built before 1986), mid-quality (built from 1986 to 2005), and high-quality (built after 2006). Based on the number of stories, the residential buildings of District 2 fall into three height classes, as shown in Table (3).

As the vulnerability curves of were adopted from Fallah-Tafti et al. [21], the same building height and construction time classification brackets

Table 3. Building classification according to height.

Building Height	Number of Stories
Low-Rise	1-3
Mid-Rise	4-7
High-Rise	More than 7

were used as a proxy for construction quality. As such, the exposure and vulnerability models could be related to the loss calculation process.

Considering classifications of construction type, year built, and the number of stories and excluding non-existent combinations, 29 vulnerability classes of residential buildings were defined for District 2 of the Tehran municipality. Table (4) exhibits the vulnerability classes of residential buildings in District 2, and Figure (7) shows how these different classes are distributed in the District.

2.3. Vulnerability Functions

A fragility function defines the probability of exceeding damage states in a set of ground motion levels, and a vulnerability function indicates the ratio or percentage of loss for ground motion levels for a given vulnerability class. In this paper, the fragility functions developed by Fallah-Tafti et al. [21] in 2020 and Mansouri et al. [18] in 2014 for common Iranian buildings are used for damage and loss calculations because they were compatible with the classification used for residential buildings in the study area. The priority has been given to fragility curves developed by Fallah-Tafti et al. [21] since their research was more recent than other studies. However, in cases where no fragility curve was available for certain classes of buildings, curves were sought from work done by Mansouri et al. [18]. After reaching a complete set of fragility functions for all classes of buildings, the fragility curves were converted to vulnerability functions using representative loss ratio for each damage state as described by the Technical Manual of HAZUS methodology for earthquake risk assessment [35]. For each building class, fragility and vulnerability functions were adopted from two recent studies and further processed to produce for other building classes, and the results were used in the risk assessment process. Figure (8) represents examples of vulnerability curves

Table 4. Building classification for residential buildings in the study area.

Building Type	Building Height	Building Quality	Building Code
Reinforced Concrete	Low-Rise (1-3 Stories)	Low-Quality (Before 1986)	R_LR_LQ
		Mid-Quality (1986-2006)	R_LR_MQ
		High-Quality (After 2006)	R_LR_HQ
		Unknown	R_LR_U
	Mid-Rise (4-7 Stories)	Low-Quality (Before 1986)	R_MR_LQ
		Mid-Quality (1986-2006)	R_MR_MQ
		High-Quality (After 2006)	R_MR_HQ
		Unknown	R_MR_U
	High-Rise (More than 7 Stories)	Mid-Quality (1986-2006)	R_HR_MQ
		Unknown	R_HR_U
Steel Structure	Low-Rise (1-3 Stories)	Low-Quality (Before 1986)	S_LR_LQ
		Mid-Quality (1986-2006)	S_LR_MQ
		High-Quality (After 2006)	S_LR_HQ
		Unknown	S_LR_U
	Mid-Rise (4-7 Stories)	Low-Quality (Before 1986)	S_MR_LQ
		Mid-Quality (1986-2006)	S_MR_MQ
		High-Quality (After 2006)	S_MR_HQ
		Unknown	S_MR_U
	High-Rise (More than 7 Stories)	Mid-Quality (1986-2006)	S_HR_MQ
		Unknown	S_HR_U
Concrete or Steel Structure*	Low-Rise (1-3 Stories)	Low-Quality (Before 1986)	SR_LR_LQ
		Mid-Quality (1986-2006)	SR_LR_MQ
		Unknown	SR_LR_U
	Mid-Rise (4-7 Stories)	Low-Quality (Before 1986)	SR_MR_LQ
		Unknown	SR_MR_U
	High-Rise (More than 7 Stories)	Unknown	SR_HR_U
Masonry	Low-Rise (1-3 Stories)	Low-Quality (Before 1986)	M_LR_LQ
		Unknown	M_LR_U
Adobe	Low-Rise (1-3 Stories)	Unknown	A_LR_U

*: The "concrete or steel structure" building type is one of the construction types used in the exposure data acquired from the Tehran Disaster Management and Mitigation Organization (TDMMO). The type has been used on occasions where concrete and steel structures were ambiguous. As a solution to overcome this challenge, a new vulnerability curve was developed by combining curves for concrete and steel structure building types using equal weights.

Figure 7. Distribution of residential building in the study area.

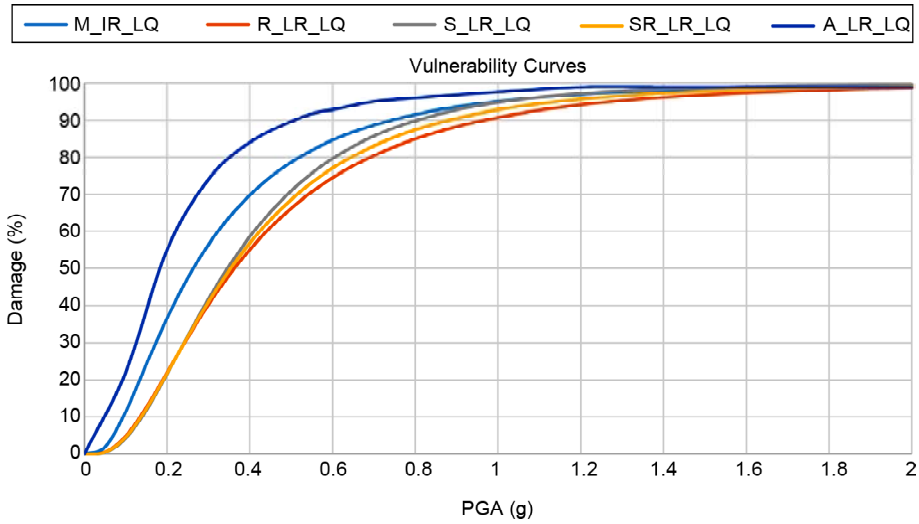

Figure 8. Examples of vulnerability curves adopted for the study region for low-rise and low-quality building types.

generated in this study. Due to the results, the most vulnerable building type was adobe and the most resistant building type was concrete.

2.4. Scenario Risk Assessment

A scenario seismic risk assessment was performed for the residential buildings in District 2 of Tehran city using the calculation platform of OpenQuake for a magnitude 6.1 earthquake generated by a rupture in the North Tehran Fault (NTF). To this end, the hazard, vulnerability and exposure components developed earlier were utilized. The risk assessment output includes the average area loss for each residential building existing in the exposure model. The damage ratio of each building was calculated by dividing area loss by the total built area. In the case the average loss ratio exceeds 0.6, the total loss is assumed. Figure (9) illustrates the damage percentage distribution in the study area. As it is noticeable in the maps, the distribution of damaged buildings is dispersing. The northern parts of the District have been more damaged because of their vicinity to the seismic source. However, due to locating of more vulnerable types of buildings, such as masonry and adobe construction, in the southern portions of the study area, high damage ratios are still observable in the south. In addition, there are more minor damages in recently constructed buildings that are more resistant.

To estimate the economic loss of the earthquake scenario, the loss ratio is multiplied by the replacement cost of the damaged building class. In case of a total loss, extra costs for demolishing the building should be added to the loss. The methodology employed for estimating the demolition cost is provided in the next section.

To recognize the replacement cost value, another field survey was conducted, through interviews with real estate agencies in different parts of District 2. The average replacement cost value for the calculations was utilized. It should be noted that only one replacement cost value was calculated for each building type and not one for each damage state because the average damage ratio (which is a weighted average of four damage state ratios) was used in the loss calculations.

2.4.1. Estimation of the Demolition Cost

Generally, the demolition cost depends on various factors such as construction material, demolition method, ceiling type, number of stories, location of the building, construction year, and the like. According to Directive No. 30129/1999/160,9 (2015), the costs of monitoring, collecting, transporting, and disposal of each m3 of construction and demolition waste are calculated based on the following formula and recommendations.

$$c = cm\left(vs \times s_1\right) + 1.4\left(s_2 \times h\right) \times ed \qquad (1)$$

In this formula, '*c*' is total demolition cost (IRR), 'cm' is the ongoing cost of the services (IRR), '*Vs.*' is the demolition waste volume, 'S1' is the demolition area (m^2), 'S_2' is the lowest level of the excavation

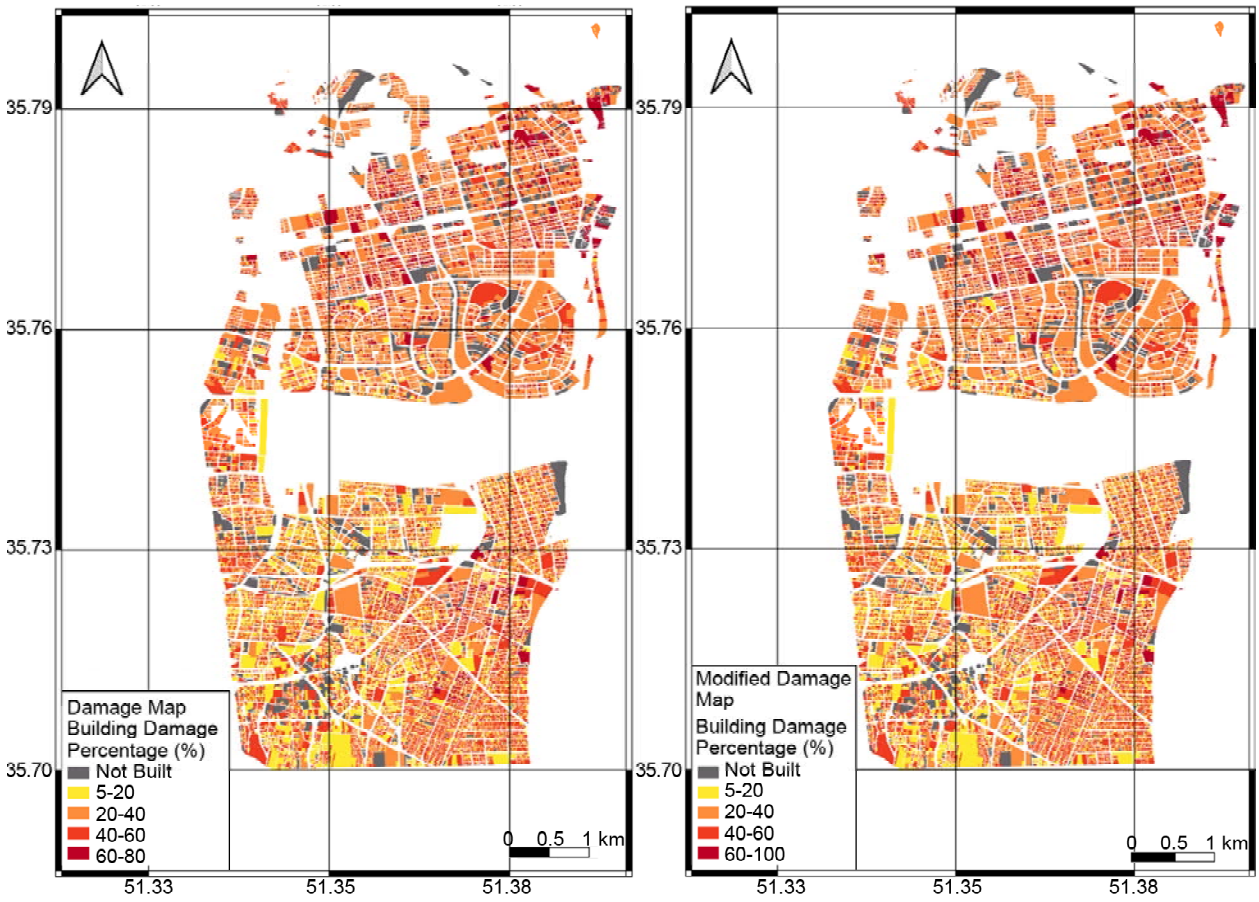

Figure 9. Distribution of damage for residential buildings in District 2 of Tehran municipality.

area (m^2), '*h*' is excavation height (m), and '*ed*' is the regional modular coefficient that is one for District 2.

3. Discussion and Conclusion

This paper provides information on the process of seismic hazard and risk (probable loss) assessment in District 2 of Tehran as a prerequisite information for disaster risk management planning (e.g. emergency planning, needs assessment, building rehabilitation prioritization, reconstruction planning, etc.) in urban areas with similar size and seismicity level in Iran. In this study, a scenario earthquake risk assessment was carried out for residential buildings in District 2 of Tehran municipality considering a 475-year event in northern Tehran, and the intensity and spatial distribution of probable losses were estimated by combining three risk components of hazard, vulnerability, and exposure. The hazard model was developed in this study using publicly available data, such as past earthquake catalogues, hazard analysis studies, and seismotectonic data, among others. The exposure model was formed by the use of national housing and population census data and past relevant research works. However, the vulnerability model was adopted from two sets of vulnerability functions previously developed for common Iranian buildings. A methodology was also devised for estimating the demolition costs for buildings experiencing destruction. The damage and loss results indicate more severe destruction in northern parts of the District where higher proximity to the earthquake epicenter exists. Nevertheless, due to the existence of more vulnerable types of buildings, such as masonry and adobe construction, in the southern margins of the study area, high damage ratios were observable in the south. Moreover, there are more minor damages in recently constructed buildings that are more resistant. To validate the risk results, each component of the risk model has been separately examined.

The earthquake loss was calculated based on the damage ratios obtained and considering the demolition costs for the building with destruction. Table (5) summarizes the aggregate results of the

Table 5. Total reconstruction cost (Exchange rate in 2021).

Number of Buildings	Total Built Area (m^2)	The Total Damaged Area Resulted from Scenario Earthquake (m^2)	Average Damage (%)	Reconstruction Cost (IRR)	Reconstruction Cost (USD)
46,924	24,445,518	7,897,023.57	32.30	395×10^{12}	1.5×10^{9}

loss estimation.

According to the results, the replacement cost of losses is estimated at IRR 395 trillion (equivalent to USD 1.5 billion) for residential building stock if a 475-year return period earthquake occurs. The value of losses is equivalent to 3 percent of the country's whole annual budget and 15 percent of the country's civil budget. Thus, because the size and population of the study area are comparable to other large-size cities in the country, the results could be used by other local governments in forming an understanding of how other similar-size urban areas could be affected by large-scale seismic events in the future.

The present study shows that the distribution and intensity of earthquake losses in this district do not only depend on the epicentral distance or event hazard distribution but also is a complicated function of vulnerability and building typology in the area which is specific to the construction practice, economy, and awareness of the population. That said, the general results of the study, namely the size of losses for the magnitude of the earthquake could be used as rough insight for disaster risk mana-gement for similar-sized cities in the country. However, the intensity and spatial distribution of losses can only be obtained after conducting numerical risk assessments in other areas. The main contribution of this paper is to address the importance of considering all risk components in risk assessment studies, which are meant to be used by decision-makers in the domain of disaster risk management.

Acknowledgments

This study is a part of the master's thesis research. The authors would like to show their gratitude to the International Institute of Earthquake Engineering and Seismology (IIEES) for their support during this research. The authors especially appreciate Tehran Disaster Mitigation and Management Organization (TDMMO) for providing the data and Islamic Revolution Housing Foundation (IRHF) for their valuable contribution.

References

1. Amini Hosseini, K., Hosseini, M., and Jafari, M.K. (2015) Recognition of vulnerable urban fabrics in earthquake zones: a case study of the Tehran. *Journal of Seismology and Earthquake Engineering*, **10**(4), p. 2009.

2. Motamed, H., Khazai, B., Ghafory-Ashtiany, M. and Amini-Hosseini, K. (2014) An automated model for optimizing budget allocation in earthquake mitigation scenarios. *Natural Hazards*, **70**(1), 51-68.

3. MunichRe, M.R.C. (2018) *NatCatSERVICE Analysis Tool*. Natural Loss Events 1980-2018, 2018. [Online]. Available: https://natcatservice.munichre.com [Accessed: 06-Apr-2022].

4. SwissRe (2018) *Swiss Reinsurance Company, SwissRe*. Natural Catastrophes [Online]. Available: https://sigma-explorer.com [Accessed: 06-Apr-2022].

5. SCI (2016) *Statistical Centre of Iran*. Tehran, SCI, formerly, the plan and budget organization of the imperial government of Iran, statistical Centre.

6. Berberian, M. (1999) Patterns of historical earthquake ruptures on the Iranian plateau. *Developments in Earth Surface Processes*, **17**(1), 439-518.

7. Ghodrati Amiri, G., Motammed, R., and Rabet Eshaghi, H. (2003) Seismic hazard assessment of metropolitan Tehran Iran. *J. Earthq. Eng.*, **7**.

8. Nowroozi, A.A. (2010) Probability of peak ground horizontal and peak ground vertical accelerations at Tehran and surrounding areas. *Pure and Applied Geophysics*, **167**(12), 1459-1474.

9. Ghafory-Ashtiany, M. (1999) Rescue operation and reconstruction of recent earthquakes in Iran. *Disaster Prevention and Management*, **8**(1), 5-20.

10. Zare, M. (2005) Seismic hazard Analysis in Tehran quadrangle. *International Institute of Seismology and Earthquake Engineering*.

11. Mirzaei, N. (2006) *Seismic Hazard Assessment and Zoning of Tehran Region*. Tehran: Tadbir Publication.

12. Zafarani, H., Noorzad, A., Ansari, A., and Bargi, K. (2009) Stochastic modeling of Iranian earthquakes and estimation of ground motion for future earthquakes in Greater Tehran. *Soil Dynamics and Earthquake Engineering*, **29**(4), 722-741.

13. Wang, J.P. and Taheri, H. (2014) Seismic hazard assessment of the Tehran region. *Natural Hazards Review*, **15**(2), 121-127.

14. Bastami, M. and Kowsari, M. (2014) Seismicity and seismic hazard assessment for greater Tehran region using Gumbel first asymptotic distribution. *Structural Engineering and Mechanics*, **49**(3), 355-372.

15. Boostan, E., Tahernia, N., and Shafiee, A. (2015) Fuzzy-probabilistic seismic hazard assessment, case study: Tehran region, Iran. *Natural Hazards*, **77**(2), 525-541.

16. Firuzi, E., Ansari, A., Amini Hosseini, K., and Karkooti, E. (2020) Developing a customized system for generating near real-time ground motion ShakeMap of Iran's earthquakes. *Journal of Earthquake Engineering*, **26**(7), 1-23.

17. Kowsari, M. and Ghasemi, S. (2021) A backbone probabilistic seismic hazard analysis for the North Tehran Fault scenario. *Soil Dynamics and Earthquake Engineering*, **144**, 106672.

18. Mansouri, B., Kiani, A., and Amini-Hosseini, K. (2014) A Platform for earthquake risk assessment in Iran case studies: Tehran scenarios and Ahar-Varzeghan earthquake. *Journal of Seismology and Earthquake Engineering*, **16**(1), 51-69.

19. Sadeghi, M., Ghafory-Ashtiany, M., and Pakdel-Lahiji, N. (2015) Developing seismic vulnerability curves for typical Iranian buildings. *Proceedings of the Institution of Mechanical Engineers, Part O: Journal of Risk and Reliability*, **229**(6), 627-640.

20. Motamed, H., Calderon, A., Silva, V., and Costa, C. (2019) Development of a probabilistic earthquake loss model for Iran. *Bulletin of Earthquake Engineering*, **17**(4), 1795-1823.

21. Fallah Tafti, M., Amini Hosseini, K., and Mansouri, B. (2020) Generation of new fragility curves for common types of buildings in Iran. *Bulletin of Earthquake Engineering*, **18**(7), 3079-3099.

22. Tavakoli, B. and Tavakoli, S. (1993) Estimating the vulnerability and loss functions of residential buildings. *Natural Hazards*, **7**(2), 155-171.

23. Japan International Cooperation Agency (JICA) (2000) *The Study on Micro Zoning of the Greater Tehran Area in the I.R. of Iran.* Final Report, Tehran, Iran.

24. Ranjbaran F. and Hosseini, M. (2012) Analytical fragility curves of confined masonry buildings. *15th World Conference of Earthquake Engineering*.

25. Kazemi, H., Ghafory-Ashtiany, M., and Azarbakht, A. (2013) Effect of epsilon-based record selection on fragility curves of typical irregular steel frames with concrete shear walls in Mashhad city. *International Journal of Advanced Structural Engineering*, **5**(1), 1-11.

26. Pakdel-lahiji, N., Hochrainer-Stigler, S., Ghafory-Ashtiani, M., and Sadeghi, M. (2015) Consequences of financial vulnerability and insurance loading for the affordability of earthquake insurance systems: evidence from Iran. *Consequences of Financial Vulnerability and Insurance Loading for the Affordability of Earthquake Insurance Systems*, **40**(2), 295-315.

27. Gardner J.K. and Knopoff, L. (1974) Is the sequence of earthquakes in southern California, with aftershocks removed, poissonian? *Bulletin*

of the Seismological Society of America, **64**(5), 1363-1367.

28. Uhrhammer, R.A. (1986) Characteristics of northern and central California seismicity. *Earthquake Notes*, **1**, 21.

29. Wiemer, S. and Wyss, M. (2000) Minimum magnitude of completeness in earthquake catalogs: Examples from Alaska, the Western United States, and Japan. *Bulletin of the Seismological Society of America*, **90**(4), 859-869.

30. Gutenberg, C.F., Richter, B. (1944) Frequency of earthquakes in California. *Bull. Seismol. Soc. Am.*, **34**, 185-188.

31. Kijko, A. (2000) Statistical estimation of maximum Regional Earthquake Magnitude m max. *Published by Elsevier Science 12th European Conference on Earthquake Engineering*, 1-22.

32. Firuzi, E., Ansari, A., Amini Hosseini, K., and Rashidabadi, M. (2019) Probabilistic earthquake loss model for residential buildings in Tehran, Iran to quantify annualized earthquake loss. *Bulletin of Earthquake Engineering*, **17**(5), 2383-2406.

33. Stewart, J.P., Eerie, M., Douglas, J., and Javanbarg, M. (2015) Selection of ground motion prediction equations for the global earthquake Model. *Earthquake Spectra*.

34. JICA (2004) *The Comprehensive Master Plan Study on Urban Seismic Disaster Prevention and Management for the Greater Tehran Area in the Islamic Republic of Iran*. The Final Main Report.

35. FEMA (1999) *Hazus -MH 2.1*. Washington, D.C.

36. Directive No. 30129/1999/160 (2015) How to calculate and get the costs of monitoring, collecting, transporting, and disposal of each m^3 of construction and demolition waste, Iran.